FAST-NEUTRON TOTAL AND SCATTERING CROSS SECTIONS OF Cr, Fe AND ^{60}Ni

by

A.B. Smith, P.T. Guenther and J.F. Whalen

Prepared for

International Conference

on

Nuclear Cross Sections for Technology

Knoxville, Tennessee

October 22-26, 1979

U of C-AUA-USDOE

ARGONNE NATIONAL LABORATORY, ARGONNE, ILLINOIS

Operated under Contract W-31-109-Eng-38 for the

U. S. DEPARTMENT OF ENERGY

DISCLAIMER

The facilities of Argonne National Laboratory are owned by the United States Government. Under the terms of a contract (W-31-109-Eng-38) among the U. S. Department of Energy, Argonne Universities Association and The University of Chicago, the University employs the staff and operates the Laboratory in accordance with policies and programs formulated, approved and reviewed by the Association.

MEMBERS OF ARGONNE UNIVERSITIES ASSOCIATION

The University of Arizona
Carnegie-Mellon University
Case Western Reserve University
The University of Chicago
University of Cincinnati
Illinois Institute of Technology
University of Illinois
Indiana University
The University of Iowa
Iowa State University
The University of Kansas
Kansas State University
Loyola University of Chicago
Marquette University
The University of Michigan
Michigan State University
University of Minnesota
University of Missouri
Northwestern University
University of Notre Dame
The Ohio State University
Ohio University
The Pennsylvania State University
Purdue University
Saint Louis University
Southern Illinois University
The University of Texas at Austin
Washington University
Wayne State University
The University of Wisconsin-Madison

FAST-NEUTRON TOTAL AND SCATTERING CROSS SECTIONS OF Cr, Fe and ^{60}Ni*

A. B. Smith, P. T. Guenther and J. F. Whalen
ARGONNE NATIONAL LABORATORY
9700 South Cass Avenue
Argonne, Illinois 60439, USA

Neutron total cross sections are measured with broad resolutions (50-100 keV) from ≈1.0-4.5 MeV at intervals of ≤50 keV and to accuracies of ≈1% using a variety of sample thicknesses. Differential elastic-scattering cross sections are measured at ≥10 scattering angles distributed between 20-160 deg. from ≈1.5-4.0 MeV at intervals of ≤50 keV. Angle-integrated elastic scattering cross sections are deduced from the measured values to accuracies ≥5%. Inelastic-neutron-scattering cross sections are determined up to incident neutron energies of 4.0 MeV, at scattering angles distributed between 20-160 deg., and for 5 observed excitations in Cr, for 7 in Fe and for 6 in ^{60}Ni. The experimental results are discussed in terms of conventional optical-statistical models with attention to cross section fluctuations and in the context of direct-scattering processes. The experimental and calculational results are compared with the corresponding evaluated quantities given in the ENDF/B file with attention to regions of agreement and inconsistency.

[Nuclear Reactions, Cr, Fe and ^{60}Ni, measured σ_T and σ_{SCAT} 1-4.5 MeV, Model interpretation.]

I. INTRODUCTION

The fast-neutron data of the primary constituents of stainless steel remain remarkably deficient and fall far short of meeting the stated need.[1] This is despite of the fact that many of the data needs in this area can be met with relatively modest applications of existing measurement systems and techniques. These observations stimulated new interest in structural-material measurements at Argonne. This report outlines results obtained in this renewed effort.

The objective was the measurement of energy-averaged neutron total and scattering cross sections of chromium, iron and nickel providing the neutron elastic-and inelastic-scattering cross sections to the requested accuracies of ≈5% over the energy range 1-5 MeV. The procedure was the measurement of broad-resolution neutron total and elastic-scattering cross sections to accuracies that imply a non-elastic cross section to an uncertainty of ≈5%. Concurrently, neutron inelastic-scattering cross sections were sought consistent with the non-elastic cross section and to the same accuracies. This procedure implies energy-averaged total neutron cross section accuracies of ≈1% and neutron elastic-scattering cross sections to accuracies of ≤5%. Generally, the detailed aspects of this work are given in the Laboratory reports of Refs. 2-5.

II. MEASUREMENT METHODS

A. Samples

All measurement samples were fabricated into cylinders from high-chemical-purity metal. The Cr and Fe samples consisted of elemental material while the Ni sample was essentially 100% enriched in the isotope ^{60}Ni. All scattering samples were approximately 2 cm in diameter and 2 cm long. The Cr and Fe total-cross-section samples varied in length so as to provide a number of transmissions over the range of 20-80%. The ^{60}Ni total cross sections were determined using the above scattering sample.

B. Neutron Total Cross Sections

The neutron-total-cross-section measurements were made using the monoenergetic-source facilities at the Argonne National Laboratory Fast Neutron Generator. The neutron source was produced by a proton burst of ≈1 nsec duration incident on a lithium metal film at a repetition rate of 2 MHz. The energy of the resulting neutrons was governed by the proton energy and the neutron-energy resolution was controlled by the thickness of the lithium-target film. A shield and associated collimator around the source were used to obtain a neutron beam ≈1 cm in diameter at a zero-degree source-reaction angle. The samples were placed upon a wheel so that they rapidly rotated through the beam. The neutron detector was a proton-recoil scintillator placed on the neutron-beam axis approximately 5 m from the neutron source. Conventional time-of-flight techniques were used to obtain the velocity spectra of neutrons arriving at the detector. Backgrounds and source perturbations were small and easily determined from an analysis of the velocty spectra. A random signal was introduced into the data acquisition system in order to precisely determine dead-time corrections. In-scattering corrections were estimated and found to be negligible. The neutron transmissions through the samples followed directly from the observed detector responses. The total cross sections were calculated from the transmissions in the conventional manner[6].

C. Neutron Scattering Measurements

The neutron scattering measurements were made using the Argonne National Laboratory 10-angle, pulsed-beam time-of-flight system using the above pulsed ^{7}Li(p,n)^{7}Be source. The mean incident-neutron energy at the scattering sample was known to ≈10 keV. The scattering samples were placed ≈13 cm from the neutron source at a zero-degree reaction angle. Proton-recoil scintillators were placed at flight paths of 5 to 5.5 m. The flight paths extended over a scattered-neutron angular range of 20 to 160 deg. The scattering angles were determined to a relative ≤0.5 deg. accuracy

*This work supported by the U. S. Department of Energy.

and to an absolute accuracy of ≲1.0 deg. The relative energy dependencies of the scattered-neutron-detector sensitivities were determined by observation of neutrons scattered from hydrogen (polyethylene) at selected angles and a fixed incident energy or from measurements of the neutron spectrum emitted during the spontaneous fission of ^{252}Cf[7]. The normalizations of the relative-detector sensitivities were determined by observing neutrons scattered from hydrogen (polyethylene) at selected energies and angles. Thus all scattering cross sections were determined relative to well known H(n,n) cross sections[8]. The measured velocity spectra were reduced to cross sections and corrected for angular resolution, sample attenuation and multiple-event effects[7]. Concurrent determinations of the elastic scattering cross sections of carbon verified the fidelity of the measurement system. In the case of ^{60}Ni there were some ancillary measurements of the (n;n', gamma) cross sections using conventional GeLi detector techniques[3].

III. EXPERIMENTAL RESULTS

A. Neutron Total Cross Sections

The objective of the total cross section measurements was the determination of precise energy-averaged magnitudes comparable with the subsequently measured scattering cross sections, model predictions and evaluations. Resolution of detailed resonance structure was explicitly avoided. The measured energy range varied somewhat from sample to sample but generally extended from 1.0 - 4.5 MeV with mesurements made at intervals of ≲50 keV with incident resolutions of >50 keV. The Cr and Fe measurements envolved at least four sample thicknesses. The experimental values for a given sample thickness were averaged over incident energy intervals of 100 - 200 keV to obtain average values with a statistical accuracy of ≈1%. The energy-averaged results were appreciably dependent upon sample thickness. The results obtained with the thicker samples were very much lower than those obtained with the thin samples due to the appreciable self shielding of the samples. The results obtained with the various sample thicknesses were extrapolated to the zero-thickness value to obtain the "true" energy-averaged cross sections. In the case of Fe carefully-measured high resolution results have been obtained by Harvey et al.[9]. In this unusual case the resolution is sufficient to resolve the structure well into the MeV range and thus the average of the high resolution results should be consistent with the present broad-resolution values. The agreement is generally within ≈1% as illustrated in Fig. 1A. On the average, both of the measured sets of values tend to be systematically larger than a corresponding average constructed from the ENDF/B-IV file. A somewhat similar trend was observed in the comparison of the measured and evaluated neutron total cross sections of Cr shown in Fig. 1B. These comparisons suggest that experimenters have not generally given proper consideration to the interplay of resolution, sample thickness and resonance structure and that, as a consequence, the neutron-total-cross-section data base in the highly fluctuating structural region may be systematically distorted to too low values in the MeV range with consequent impact upon the evaluated files. Similar problems are known to occur in other mass-energy regions.

The ^{60}Ni neutron total cross sections measurements had to be confined to a single and relatively thick sample. As a consequence the measured values are systematically lower than an equivalent average constructed from the better resolution results of Clement et al.[10] at lower energies as illustrated in Fig. 1C. Numerical estimates suggest that the present values are distorted by 5-10% (or in the extreme, 20%) toward too low values at energies below 1 MeV. This distortion rapidly decreases as the energy increases. There is no comparable ENDF/B file, but optical models based upon high-energy scattering measurements generally predict higher neutron total cross sections in this mass region near 1 MeV. The discrepancies may be due, in part, to shortcomings in the models or physical behavior such as fluctuations, "doorways"[11], etc., that are not consistent with the underlying precepts of the optical model. However, the model-measurement discrepancy has been widely observed and an extreme example is shown in Fig. 1C. Such discrepancies tend to be consistent with shortcomings in the experimental determinations of energy-averaged neutron total cross sections in this mass-energy region.

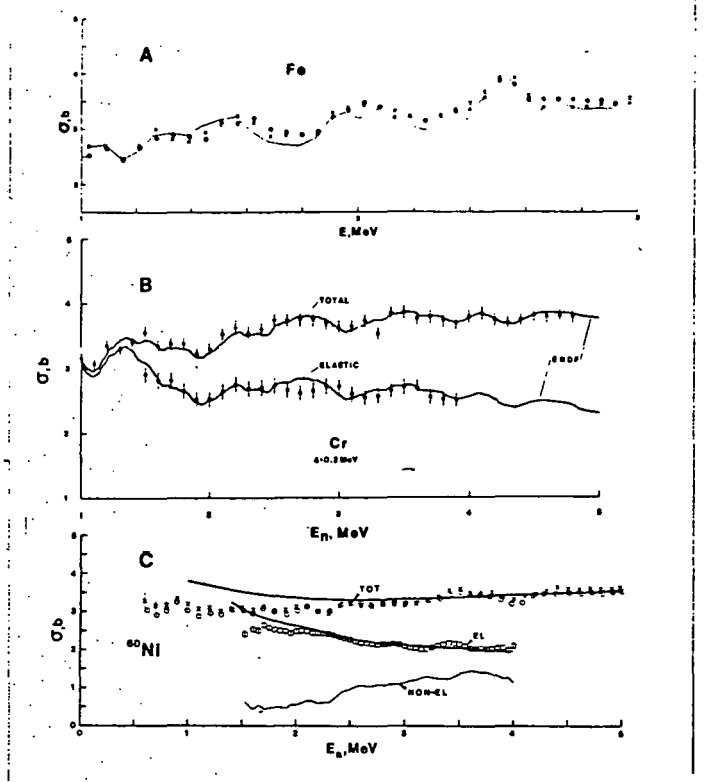

Fig. 1. Neutron cross sections of: A Iron, present total-cross-section results (O), equivalent average of the Ref. 9 values (X), and ENDF-IV (curve). B. Chromium, present total (O) and elastic-scattering (□) results, and ENDF-IV (curves). C. ^{60}Ni, Present total (O) and elastic scattering (□) results, equivalent average of total cross sections of Ref. 10 (X), and results of model calculations (heavy curves).

B. Neutron Elastic Scattering

Elastic neutron scattering cross sections were measured at incident energy intervals of <50 keV from 1.5 to 4.0 MeV with incident-energy resolutions of ≈20-60 keV. The objective was an angle-energy scope that would well define the elastic scattering cross sections to an intermediate energy resolution. The individual differential scattering cross sections were generally determined to 5 to 8% accuracies. Statistical uncertainties contributed 1-3% to the overall uncertainties. Correction procedures, including those for effects due to angular uncertainties, made a similar small contribution. The largest contribution to the overall uncertainty came from the calibration of the detector efficiency (typically 3 to 5%). The uncertainty in the H(n,n) standard was a small factor (i.e. ≲1%).

Despite the relatively-broad incident-energy resolutions, considerable variation in the distributions with energy was discernable throughout the measured energy range. Any single distribution was not necessarily representative of the more general energy-averaged behavior. A better representation of the average behavior was obtained by averaging the measured values over 200-keV intervals with results as illustrated in Fig. 2. With these 200-keV averages, the behavior of the distributions varies reasonably smoothly with energy, and is comparable with predictions of the energy-averaged models.

The 200-keV averages of the present results were least-square fitted with a Legendre polynomial expansion from which the angle-integrated elastic-scattering cross sections were derived. The accuracies of the latter were generally 3-5%, i.e. essentially dominated by the uncertainties associated with detector calibrations. Representative elastic-scattering cross sections are shown in Fig. 1B-C. The angle-integrated elastic scattering cross sections fluctuate with energy in a manner consistent with the fluctuations of the neutron total cross sections. Together the two sets of cross sections yield the non-elastic cross sections. The non-elastic cross sections were generally known to ≈5% and consistent with the directly-measured neutron inelastic scattering cross sections above 1.5-2.0 MeV.

C. Neutron Inelastic Scattering

Differential-neutron-inelastic-scattering cross sections were determined concurrently with the elastic-scattering values. Scattered neutrons were observed corresponding to levels in Cr at 1.433 ± 0.009, 2.377 ± 0.008, 2.665 ± 0.005, 2.778 ± 0.007 and 2.970 ± 0.006 MeV; in Fe at 0.853 ± 0.050, 1.389 ± 0.030, 2.097 ± 0.022, 2.579 ± 0.035, 2.677 ± 0.014, 2.974 ± 0.011 and 3.152 ± 021 MeV; and in ^{60}Ni at 1.342 ± 0.013, 2.168 ± 0.010, 2.304 ± 0.026, 2.509 ± 0.022, 2.636 ± 0.019 and 3.164 ± 0.041 MeV. These observed excitation energies are averages of a number of independent measurements and the uncertainties are RMS deviations from the mean. The presently observed excitations correspond reasonably well to previously reported levels as summarized in the compilations of Ref. 12.

Angle-integrated neutron inelastic-excitation cross sections were determined by least-square fitting no fewer than four differential values at each energy with Legendre-polynomial series. The uncertainties in the differential-cross section values ranged from a minimum of ≈5% for prominent and well-resolved neutron groups at favorable energies to $\gtrsim$20% for less well resolved and/or low-intensity neutron groups. There was a similar spread in the uncertainties of angle-integrated cross sections ranging upward from a minimum of ≈5%.

A major feature of the inelastic process is the prominent excitation of the first, 2+, levels. These levels are either vibrational (as in ^{60}Ni[12]) or rotational (as in ^{56}Fe[13]). The differential cross sections for the excitation of these levels fluctuate with energy in a manner analogous to that of the elastic scattering cross sections. In order to remove these fluctuations the measured inelastic-scattering distributions were averaged over ≈200 keV incident-neutron energy intervals in the same manner as for the elastic-scattering distributions. The resulting averages behaved in a relatively smooth manner. Furthermore, there was a trend from distributions symmetric about 90 deg. at lower energies to those that were somewhat peaked forward at upper energies in a manner that could be expected as the result of increasing contributions from direct-inelastic processes. Cross sections for the excitation of higher-lying levels also fluctuated, and averaging procedures were used to obtain the energy-averaged behavior in the same fashion as outlined above for the first, 2+, levels. Scattered neutron distributions resulting from the excitation of these higher-lying levels were generally essentially symmetric about 90 deg.

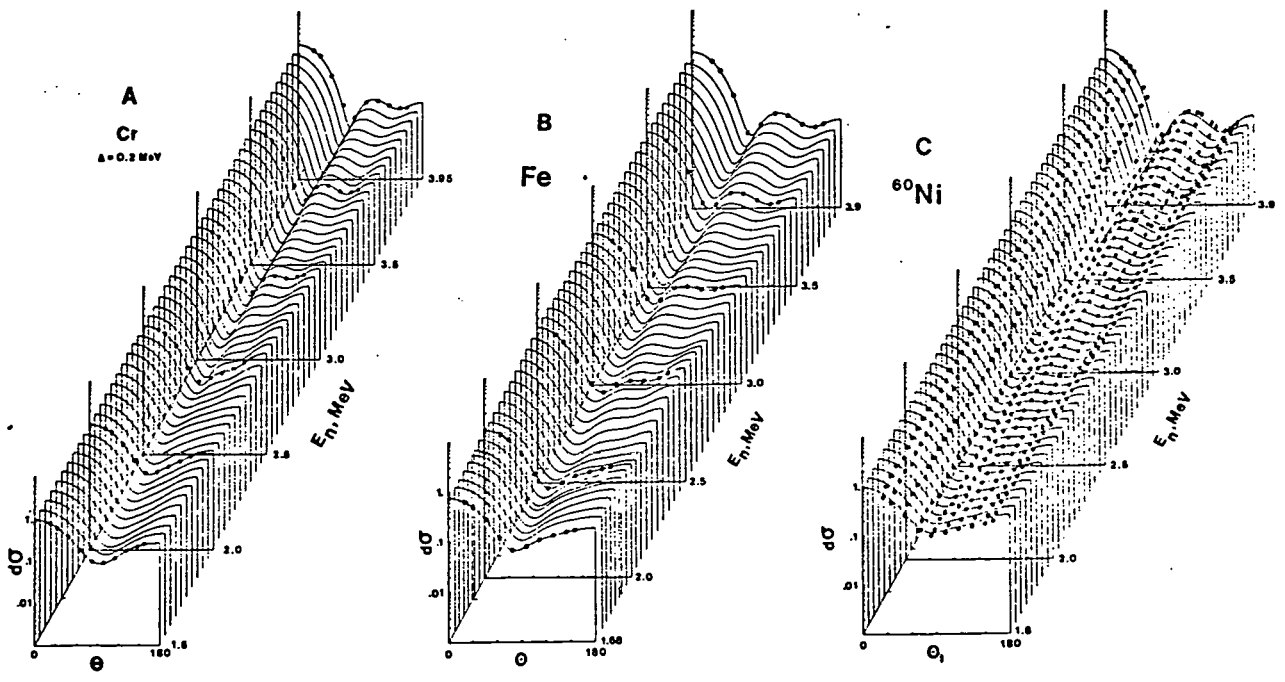

Fig. 2. Measured differential elastic scattering cross sections of chromium (A), iron (B), and ^{60}Ni (C). The present experimental results are indicated by data points. Curves denote the results of fitting Legendre expansions to the chromium and iron data and the results of model calculations in the case of ^{60}Ni. All data have been averaged over 200 keV increments.

The above direct-neutron measurements extended to within ≈0.8 MeV of threshold. In the case of ^{60}Ni, (n,n',γ) techniques were used to extend the measured cross sections for the excitation of the prominent 1.342 MeV level to threshold. The measured relative (n;n',γ) results were normalized to the directly measured (n;n') values near 2.0 MeV.

The angle-integrated neutron inelastic scattering cross sections derived from the measurements are shown in Fig. 3. There are a number of previously reported results some of which are indicated in these figures. The agreement with the present results varies from good to very poor. Many of these previous results consist of isolated or a few experimental values. The validity of comparisons of isolated values is questionable in view of the fluctuations in the cross sections and unavoidable variations in experimental energy scales and resolutions. Additional discussions of data comparisons are to be found in Refs. 3 to 5.

Many of the present neutron-inelastic-scattering results can be compared with values given in the ENDF/B-IV files, corrected to isotopic quantities where necessary. The comparisons, indicated in Fig. 3 suggest that portions of the differential inelastic scattering files are discrepant with the present results by 15-20% or more. Some of these discrepancies appear in the largest inelastic excitation cross sections (e.g. the 2+ level of iron) and amount to 5-10% (or larger) discrepancies between measured and evaluated total neutron inelastic-scattering cross sections. The present inelastic-scattering results are further supported by their consistency with the above non-elastic cross sections to within ≈5%, i.e. to within the experimental uncertainties.

IV. INTERPRETATION

The theoretical interpretations sought to: a) establish spherical optical potentials providing an acceptable description of the energy-averaged neutron cross sections in this mass-energy region of strong fluctuations, and b) explore the effect of direct-inelastic processes in the neutron interaction. The scope and detail of the present experiments provides a suitable foundation for such investigations.

The spherical optical potential was entirely based upon the 200 keV averages of the measured differential elastic-scattering cross sections. The averaging increment was a compromise between a representation consistent with the concept of the optical model and the excited-level spacing influencing the compound-elastic component. The initial step in the deduction of the potential was a 6-parameter (real and imaginary strengths, radii and diffusenesses) Chi-square fit of a conventional surface-absorption optical potential to each of the measured elastic-scattering distributions. The compound-elastic contributions were calculated using the Hauser-Feshbach formula with width-fluctuation corrections[14,15]. The initial fitting procedures reasonably defined real and imaginary radii and diffusenesses. These four-parameters were then fixed for subsequent and more detailed two-parameter (real and imaginary strengths) Chi-square fitting procedures. The latter included the enhancement of compound-nucleus components using the formalism of Hofmann et al.[16]. The level-density-distribution of Gilbert and Cameron[17] was used for the description of levels with excitations of ≳3.0 MeV. The resulting V (real strength) and W (imaginary strength) followed a general linear energy dependence. Superimposed on these general trends were relatively small (≈ ± 1 MeV) fluctuations with a periodicity of ≈0.5 MeV. These fluctuations reflected those of the underlying data bases. The fluctuations were not characteristic of a general energy-averaged behavior and were ignored in the resulting "general potentials" derived for each target. These "general potentials" were the basis for subsequent comparisons of measured and calculated values and the investigation of direct-vibrational processes. The numerical potential parameters are given in Refs. 3-5. It must be stressed that these potentials are pragmatic parameterizations of the particular experimental results and are not "global" or even "regional". Indeed, there are pronounced differences between the potentials. These differences may well be rooted in the nature of the cross section fluctuations inherent to each target. However, the "general potentials"

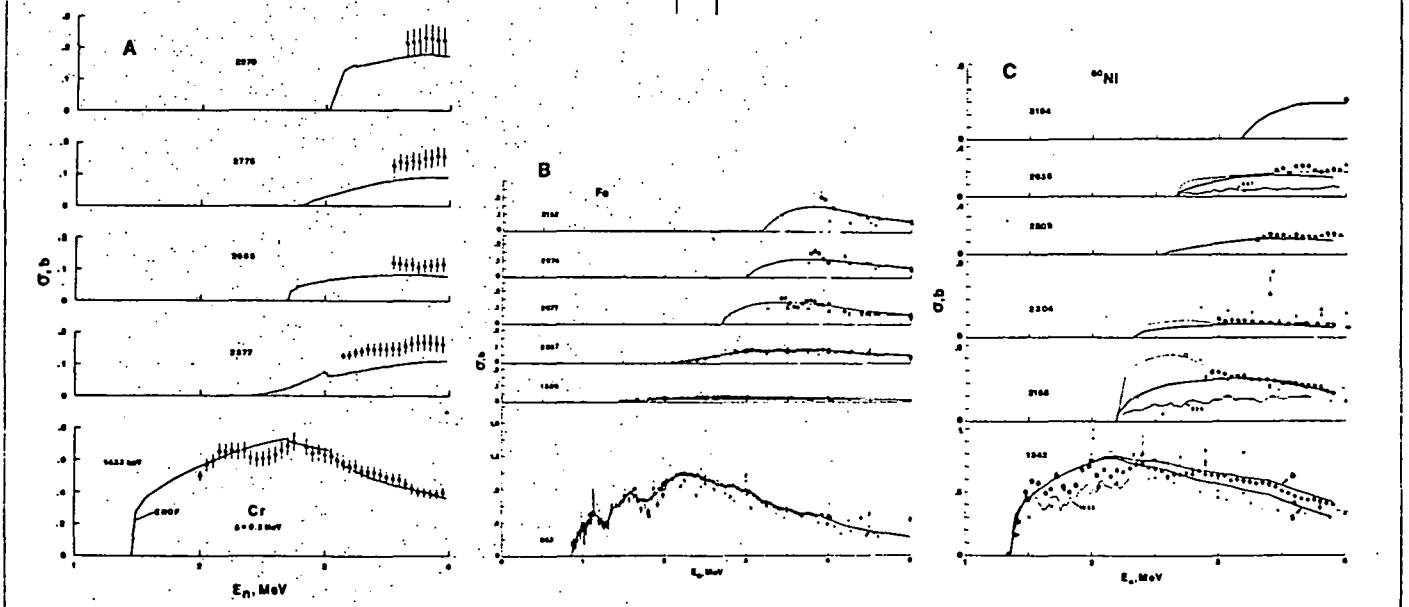

Fig. 3. Measured inelastic-neutron-excitation cross sections of Cr (A), Fe (B) and ^{60}Ni (C). The present results are indicated by solid data points. Corresponding ENDF-IV values are noted by dotted (Fe and ^{60}Ni) and solid (Cr) curves. Spherical (S or no notation) and deformed (D) model results for ^{60}Ni are indicated by solid curves.

provide an acceptable description of measured neutron-elastic-scattering cross sections of each target as illustrated in Fig. 2C. Differences between measured and calculated results were generally small and ramdom in nature as might be expected from the residual fluctuations and doorway configurations[11].

Comparisons of measured and calculated neutron total cross sections follow the same general trends as those of the angle-integrated elastic-scattering cross sections. In addition to the effects of fluctuations and doorway levels there were the problems of experimental sample-size perturbations outlined above. The differences between measured and calculated values were generally within the range of estimated experimental perturbations alone. The inability of optical potentials based upon higher-energy elastic scattering to describe neutron total cross sections near 1.0 MeV in this mass region has long been observed. As outlined above, much of this discrepancy may be experimental in origin, but there may also be a shortcoming in the concept of a simple spherical optical potential. In either event, there remains an uncertainty in energy-averaged neutron total cross sections in this mass-energy region of ≈10% in a number of nuclides.

The neutron-inelastic-scattering cross sections calculated using the spherical "general potentials" were qualitatively descriptive of the measured values (as illustrated in Fig. 3C) but there were quantitative discrepancies. The calculated excitation of the first, 2+, levels tend to be larger than the measured values below ≈2.5 MeV and smaller above ≈3.0 MeV. These differences are ≈10-30%. In addition, the calculated angular distributions of scattered neutrons do not show the forward peaking observed at higher energies. Some of the comparisons between measured and calculated excitation cross sections do suggest reconsideration of some previously assigned J-π values (see Refs. 4-5).

At higher incident energies (e.g. $\gtrsim$3.0 MeV) the above spherical interpretations have three shortcomings: a) the calculated excitations of the first, 2+, levels are systematically smaller than the measured values, b) measured neutron distributions resulting from the excitation of the first, 2+, levels are not symmetric about 90 deg. as predicted by theory, and c) the measured elastic-neutron distributions deviate systematically from the calculated values as 4.0 MeV is approached. It is difficult to attribute these shortcomings entirely to fluctuations and/or the level-density approximation employed in the calculations. However, qualitatively the above features are characteristic of direct-inelastic processes. Coulomb-excitation, (γ,n) and stripping studies indicate that the first excited, 2+, levels are rotational (e.g. ^{56}Fe) or vibrational (e.g. ^{60}Ni) states. The effects of these direct interactions were estimated using a coupled-channels calculation, coupling the ground (0+) and first-excited state assuming the β_2 values of Ref. 18. In doing so it was assumed that direct and compound-nucleus processes were approximately separable and that the latter could be reasonably calculated using transmission coefficients derived from the spherical potential. The "general potentials" were used for the direct calculations except for the imaginary strengths which were adjusted to improve the description of the observed differential elastic-scattering distributions. The direct calculations were an approximation in that they did not derive transmission coefficients directly from the deformed potential nor was there an attempt made to explictly Chi-square fit the measured elastic distributions using the deformed potential. Such procedures would have been very costly and deceptive if applied to only a few measured distributions.

The coupled-channels results mitigated the shortcomings of the spherical calculations. The calculated distributions of neutrons resulting from the excitation of the first, 2+, level were peaked forward in the manner of the measured values. The inelastic cross section magnitudes and the neutron differential-scattering distributions were in much better agreement with the measured values than those obtained from the spherical calculations (as illustrated in Fig. 3C). Thus the comparisons of measured and calculated values suggest that direct-inelastic processes are significant in the present energy range. In particular they account for facets of the interaction not consistent with the spherical optical-statistical model. Consideration of direct-inelastic interactions does result in modifications of potential parameters relative to the spherical model (e.g. 30% reduction in imaginary strength.

REFERENCES

1. WRENDA 74, IAEA Report, INDC(SEC)-38/U (1974).
2. A. Smith and J. Whalen, Argonne Natl. Lab. Report, ANL/NDM-33 (1977).
3. A. Smith et al., Argonne Natl. Lab. Report, ANL/NDM-44 (1979).
4. A. Smith and P. Guenther, Argonne Natl. Lab. Report, ANL/NDM-47 (1979).
5. P. Guenther et al., Argonne Natl. Lab. Report, to be published.
6. D. Miller, Fast Neutron Physics, Vol.-II, Inter. Sci. Pub., New York (1963).
7. P. T. Guenther, University of Ill. Thesis (1977).
8. J. Hopkins and G. Breit, Nucl. Data, A9 137 (1971).
9. J. A. Harvey et al., Data available from the NNDC.
10. Clement et al., Data available from the NNDC.
11. S. Cierjacks and I. Chouky, Proc. Conf. Neut. Data of Structural Materials for Fast Reactors, Pergamon Press, London (1979).
12. Nuclear Data Sheets for the respective masses.
13. H. E. Jackson, Priv. Com. (1979).
14. W. Hauser and H. Feshbach, Phys. Rev., 87 366 (1952).
15. P. A. Moldauer, Phys. Rev., C11 426 (1978).
16. H. Hofmann et al., Ann. Phys. (NY), 90 403 (1975).
17. A. Gilbert and A. Cameron, Can. Jour. Phys., 43 1446 (1965).
18. P. Stelson and L. Grodzins, Nucl. Data, A1 21 (1965).